



OPEN

Research on series arc fault detection method household loads based on voltage signals

Bin Li, Jiahui Shu[✉] & Feifan Cui

In order to accurately detect series arc fault, this paper proposes a series arc fault detection method based on voltage signal which introduces inception with multi-scale parallel convolution operation, and combines bidirectional long short-term memory recurrent network (BiLSTM) with attention mechanism. Firstly, a household experimental platform was built, and the line voltage signal obtained by the experiment was subjected to wavelet transform and principal component analysis (PCA) dimensionality reduction to construct a dataset. Secondly, Inception is introduced to extract the multi-level features of the samples, and the parallel output is input into BiLSTM after global max pooling layer. Then, self-attention is used to perform reinforcement learning on the hidden state vector. Finally, the output results are classified by the fully connected layer. Compared with the detection results of various algorithms, it is verified that this method has more advantages in the identification of series arc fault. In addition, additional experiments at different sampling frequencies show that the method has good adaptability, and the identification accuracy has better performance when the sampling frequency is 10 KHZ, which has certain theoretical guiding significance for the development of the series arc fault detection device in the next step.

Keywords Series arc fault detection, Multi-scale parallel convolution operation, Wavelet transform, Principal component analysis dimensionality reduction, Bidirectional long short-term memory recurrent network, Self-attention

According to the data released by the National Energy Administration, social electricity consumption has continued to rise in recent years, so the security risks increases too. According to the statistics of the Chinese National Fire and Rescue Administration, in 2022, the national fire and rescue team received a total of 825,000 fires, with 2053 deaths, 2122 injuries, and direct property losses of 7.16 billion yuan. Among them, electrical fires accounted for more than 30%. Fires that have occurred due to faulty arcs account for 75 percent of electrical fires¹. In Europe and North America, series arc faults are regarded as a significant hidden danger leading to building fires. According to the national fire protection association (NFPA) in the United States, electrical fires cause numerous casualties and substantial property damage each year, with a portion attributed to series arc faults. As a result, both regions have established legislation and standards to enhance safety protection against such hazards. In the United States, the National Electrical Code (NEC) has gradually required the installation of arc fault circuit interrupters (AFCIs) in areas such as bedrooms and living rooms since 2002. One of the primary functions of AFCIs is to detect arc faults, including series arcs. In Europe, IEC implementation standards have promoted the use of arc fault detection devices (AFDDs), particularly in high-risk environments such as schools, nursing homes, and wooden structures, to prevent potential dangers caused by series arc faults. In residential buildings, arc can be generated in electrical circuits due to short circuit, overload, poor contact, fault, improper use, etc. When an arc occurs, the temperature of the arc core can reach more than 5000 °C an electric arc generates extremely high heat, accompanied by intense light and loud noise, which can ignite nearby materials and lead to serious fires².

In order to effectively prevent and contain residential fires, the research on arc faults of various low-voltage loads has received extensive attention in recent years, and the research on detection of series arc fault has received great attention.

The first is based on the physical characteristics of arc faults for arc detection research. Vasile³ proposed an arc fault detection and localization method based on electromagnetic acoustic sensing system, combine the characteristics of the multiple emission of arc fault with real-time detection signal processing method to realize arc fault identification. Hui⁴ detected the arc voltage signal, current signal and arc light intensity signal

Faculty of Electrical and Control Engineering, Liaoning Technical University, Huludao 125105, China. [✉]email: 1043069285@qq.com

respectively, and made a soft decision based on Bayesian information fusion, so as to obtain the best arc fault judgment. However, Due to the inflexibility of the installation position of such arc fault monitoring sensors, it is difficult to effectively detect arc faults in low-voltage load lines.

Secondly, using the time-frequency domain characteristics of voltage and current waveforms to detect arc faults. Jimmi Lezama⁵ pointed out that the crest factor, skewness and kurtosis coefficient of the series current waveform can be used as the time-domain characteristics of the arc fault by using the time-domain analysis method. James⁶ used fast Fourier transform to decompose the monitored voltage and current signals into a series of detailed spectral components, and then used neural network to detect arc faults.

With the rapid rise of artificial intelligence, the use of deep learning algorithms has opened up new ideas for the detection of arc fault in lines. Jiang⁷ extracted different aspects of arc features through time domain, frequency domain and wavelet packet energy analysis, and then adopted a random forest-based feature selection method to select the top ten features closely related to arcs and feed it into a deep neural network for arc recognition. Zhang Shuai⁸ used the multi-layer discrete wavelet analysis method to analyze arc faults with different loads. The resulting five-layer discrete wavelet detail values are fused and then the coefficient matrix is converted to a phase space image indexed by a colormap. The classification data set generated by the phase space feature map is input to ResNet for convolution and classification recognition in the form of three channels. Long⁹ proposed to connect the Fourier coefficients, Mel frequency cepstral data and wavelet coefficient data as features, and import them into a deep neural network to distinguish between normal current and fault current.

Due to the excellent feature extraction ability of convolutional neural network¹⁰⁻¹⁴. Here we propose a deep learning algorithm combining Inception module containing multi-scale parallel convolution operation and BiLSTM containing attention mechanism. The specific block diagram of using this algorithm for series arc fault identification is shown in Fig. 1

Since the voltage signal related to arc fault is usually disturbed by noise, in order to better highlight the effective features and reduce the influence of background noise. In this paper, wavelet transform is performed on the voltage signal. At the same time, PCA is used to reduce the dimension of the multi-dimensional vector recombined from the original data¹⁵, the low-frequency components and the high-frequency components of each layer after wavelet transformation, and the eigenvectors with larger contribution rate are retained. With the help of multi-scale convolution operation to extract the deep effective features of the input, BiLSTM is used to extract the correlation features between different moments of the signal. During model training, the attention mechanism is introduced into the hidden state vector of each unit of BiLSTM, so that each update iteration can more efficiently increase the weight of effective features, thereby amplifying the gap between effective features and background noise, and improving the model's performance.

Introduction to theory

Introduction to the Inception module

The Inception module with deeper and wider parallel convolution computing capabilities is shown in Fig. 2, which has more prominent advantages in mining the deep features of the input signal and expanding the receptive field¹⁶.

The Inception module has four parallel channels. Features at different spatial dimensions are extracted through 1×1 , 3×3 and 5×5 convolution operations. Adding 1×1 convolutional layers before $3 \times 3/5 \times 5$ can reduce the number of input channels and reduce model complexity¹⁷. Appropriate padding is used for each channel so that the input and output are same in height and width. Finally, the convolution results on each channel are concatenated on the output channel.

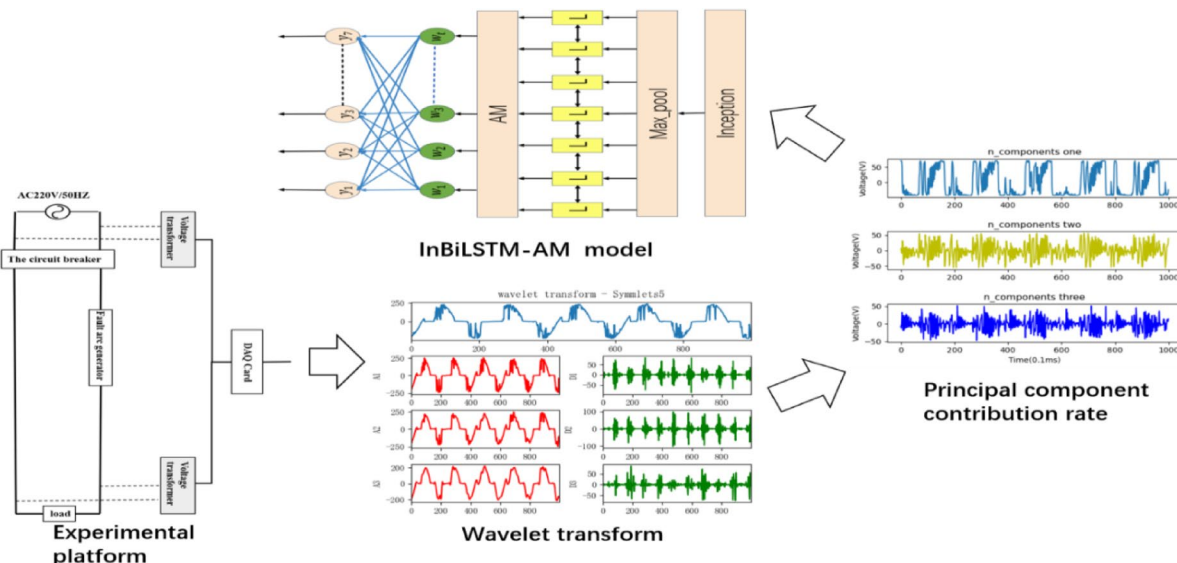


Fig. 1. Algorithm block diagram.

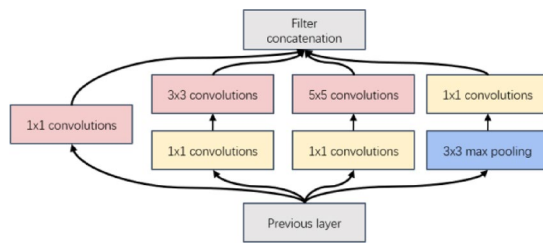


Fig. 2. Inception module.

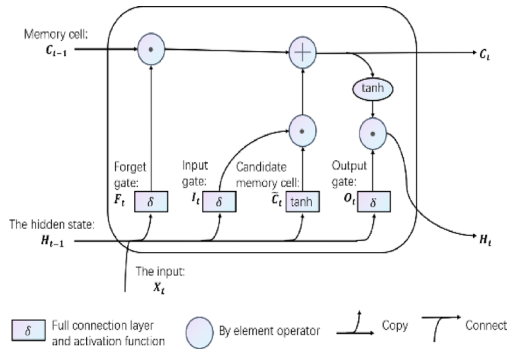


Fig. 3. LSTM module.

Introduction to LSTM

The core of LSTM is the cell state and the “gate” structure¹⁴. Its specific structure is shown in the Fig. 3 below:

The calculation formula of input gate $I_t \in R_{n \times h}$ (the number of samples is n , the number of hidden states is h), forget gate $F_t \in R_{n \times h}$ and output gate $O_t \in R_{n \times h}$ at time step t are as follows:

$$I_t = \delta(X_t W_{xi} + H_{t-1} W_{hi} + b_i) \quad (1)$$

$$F_t = \delta(X_t W_{xf} + H_{t-1} W_{hf} + b_f) \quad (2)$$

$$O_t = \delta(X_t W_{xo} + H_{t-1} W_{ho} + b_o) \quad (3)$$

Control the flow of information through the memory cell $C_t \in R_{n \times h}$ gate at the current time step

$$C_t = F_t \Theta C_{t-1} + I_t \Theta C_t \quad (4)$$

Control the flow of information from memory cells to the hidden state $H_t \in R_{n \times h}$ through output gates:

$$C_t = F_t \Theta C_{t-1} + I_t \Theta C_t \quad (5)$$

In general, LSTM controls the information forgetting and memorizing new information in the cell state, thereby the information that is valid for the calculation results of the subsequent moments is transmitted, while the invalid information is discarded.

Introduction to the BiLSTM

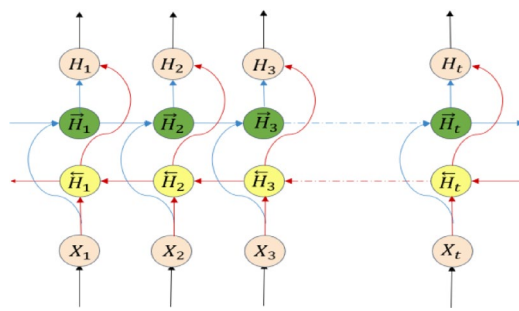
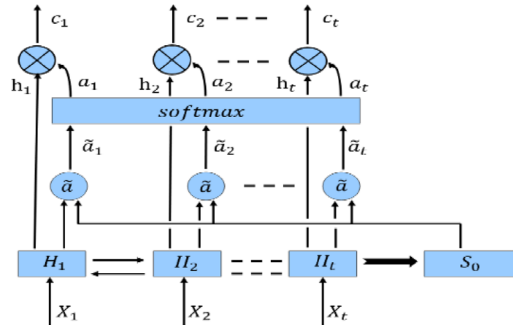
As shown in the Fig. 4 below. In order to better capture the bidirectional feature dependence of time series signals, the BiLSTM module is introduced, which is composed of a combination of forward LSTM and backward LSTM¹⁸.

The forward hidden state and reverse hidden state at time step t are calculated as:

$$\vec{H}_t = \emptyset(X_t W_{xh} + \vec{H}_{t-1} W_{hh} + b_h) \quad (6)$$

$$\overleftarrow{H}_t = \emptyset(X_t W_{xh'} + \overleftarrow{H}_{t+1} W_{h'h} + b_{h'}) \quad (7)$$

Then connect the hidden states \vec{H}_t and \overleftarrow{H}_t in both directions to get the hidden state $H_t \in R_{n \times 2h}$ as the output vector. Therefore, the hidden state of BiLSTM at each time step depends not only on the input of the current time step, but also by the subsequence information before and after the time step.

**Fig. 4.** BiLSTM module.**Fig. 5.** Self-attention mechanism.

Introduction to self-attention

As shown in the Fig. 5 below. In order to more accurately retain and filter out the effective feature information¹⁹, the attention mechanism is used to perform reinforcement learning on the hidden state vector of BiLSTM.

The first is to import the mini-batch input $X_t \in R_{n \times d}$ (sample length is d) into BiLSTM to obtain a set of hidden states $H_t \in R_{n \times 2h}$, where the hidden state at the current moment is set to S_0 , A set of weight parameters $\tilde{a}_t \in R_{n \times 2h}$ is obtained by performing \tilde{a} function operation on S_0 and the hidden state H_t of each time step, and then this set of weights is normalized to obtain the attention weight vector $a_t \in R_{n \times 2h}$, the specific operation process can be summarized as:

Step 1: Take S_0 and H_t as input vectors, and introduce two parameter matrices to linearly transform the input vector to obtain two vectors k_t, q_0 , where the parameter matrices W_t and W_0 are learned and optimized in the training data.

$$k_t = W_t * H_t \quad (8)$$

$$q_0 = W_0 * S_0 \quad (9)$$

Step 2: Do the inner product of the resulting vector to obtain a weight parameter vector \tilde{a}_t of the same length as the hidden state.

$$\tilde{a}_t = k_t^T * q_0 \quad (10)$$

Step 3: Perform the softmax operation on the weight parameter vector \tilde{a}_t to obtain the attention weight vector a_t .

$$a_t = softmax(\tilde{a}_t) \quad (11)$$

Multiply the attention weight vector with the corresponding elements of each hidden state to obtain a set of vector sequences $c_t \in R_{n \times 2h}$, Obviously, the sequence contains the feature information of each time step and the weight of each feature for the current time step.

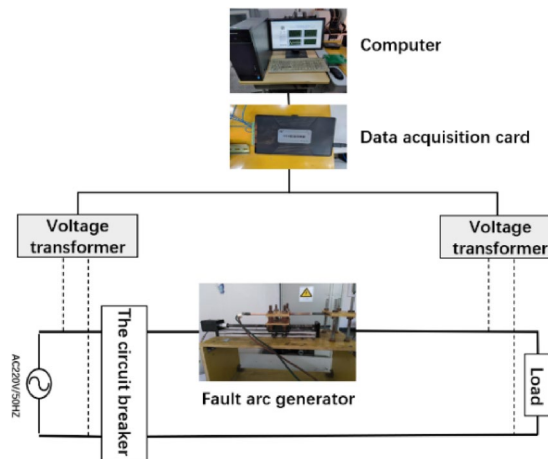


Fig. 6. Experimental platform.

Serial numbers	Experimental group	Load type	Power
1	1–2	Induction cooker	1000 W
2	3–4	Electric fan	40 W
3	5–6	Electric blanket	100 W
4	7–8	LED	20 W
5	9–10	Heater	300 W
6	11–12	Washer	200 W

Table 1. Load parameters and experimental scheme.

Data preprocessing

Experimental scheme

Regarding the structure of the experimental platform, the power port is connected to the single-phase load after the circuit breaker, and the arc fault generator is connected in series in the line. Voltage transformers are connected in parallel at the power supply side and the load side respectively to record the voltage waveform changes of the corresponding terminals under normal and fault conditions of the circuit. Finally, the collected voltage signal is transmitted to the computer through the data acquisition card, and the data is displayed and stored by LabVIEW software. The structure of the series arc fault experimental platform is shown in the Fig. 6.

The power supply used in this experiment is standard household AC 220 V/50HZ, and copper stranded wire is used as the power supply line of the main circuit. Six kinds of household loads are selected as experimental loads, including resistive, inductive and capacitive loads. Each group of experiments lasts 5 min, and a total of 12 groups of experiments are set up. The load types, parameters and specific schemes of the experiments are as shown in the Table 1.

Experimental data analysis

When the sampling frequency is 10KHZ, the data of power supply terminal voltage and load terminal voltage under different loads are obtained through experiments.

It can be analyzed from Fig. 7 that when an arc occurs, the voltage at the load terminal is greatly affected by the arc, and there will be obvious disturbance changes compared to the voltage waveform at the power supply terminal. The power supply terminal connected to the grid can be regarded as a constant current source, so the power supply terminal is less affected by the arc.

In the case of sampling time synchronization, the difference between the voltage at the power supply terminal and the voltage at the load terminal is recorded as the line voltage, and some line voltage data of various loads are intercepted and displayed as follows: the horizontal direction represents the time t (ms), and the vertical direction represents the voltage U (V).

It can be seen from Fig. 8 that in the normal state, the line voltage is very small, which is basically equal to the voltage division of the line resistance, and the line voltage fluctuates very little, only due to the interference caused by the incomplete synchronization of sampling. When a series arc fault occurs, the line voltage value is the sum of line resistance divided voltage and the arc divided voltage, the degree of waveform distortion is more obvious, the amplitude change is more severe, and it is often accompanied by zero-break phenomenon.

Obviously, the line voltage is greatly affected by the arc, and there is an inherent characteristic relationship between the two. Therefore, this paper selects the line voltage signal to detect the series arc fault.

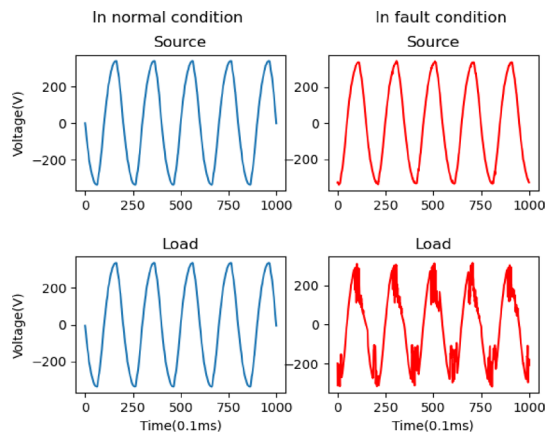


Fig. 7. Voltage waveforms at the power supply and load terminals.

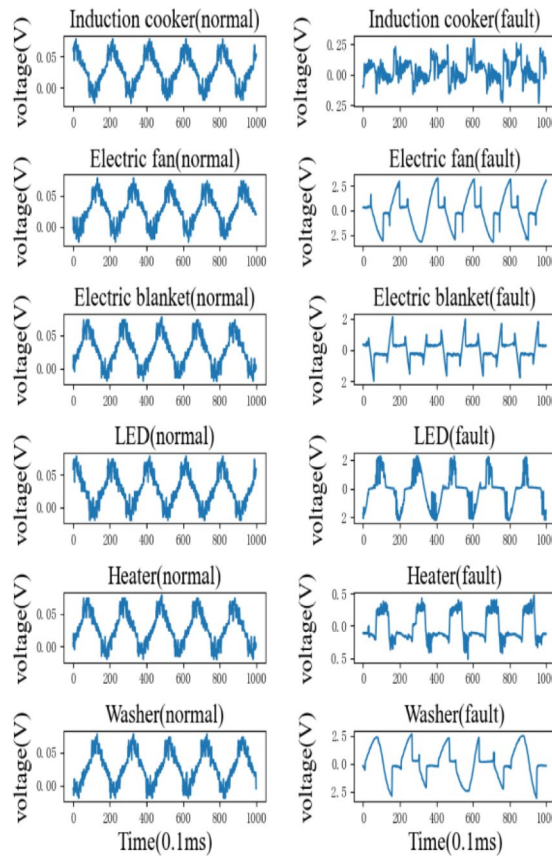


Fig. 8. Line voltage waveform of each load. (a) Normal state. (b) Fault state.

Wavelet transform

Because the time domain signal has the characteristics of being disturbed by noise and difficult to detect²⁰, this paper uses wavelet transform to analyze and mine the time–frequency domain characteristics of the signal. The principle is as follows:

$$\varphi_{j,k}(t) = a_0^{-\frac{j}{2}} \varphi(a_0^{-j}t - kb_0) \quad (12)$$

The discrete wavelet transform of $z(t)$ is defined as:

$$C_{j,k} = \int_{-\infty}^{+\infty} z(t) \varphi_{j,k}(t) dt \quad (13)$$

The discrete wavelet reconstruction formula is:

$$z(t) = \sum_{j \in Z} \sum_{k \in Z} C_{j,k} \varphi_{j,k}(t) \quad (14)$$

A single-branch reconstruction is performed on the approximation coefficients A and the detail signal D of multiple layers. Here is an example of the LED lamp fault circuit as follows.

It can be seen from Fig. 9 that the mutation region of the high-frequency component of the line voltage signal is stable, and its low-frequency component can retain the characteristics of the voltage signal of the load itself.

PCA dimensionality reduction

PCA is a linear dimensionality reduction algorithm²¹, which can calculate new variables that contain a certain proportion of the original information and are independent of each other. The principle can be summarized as:

Assuming that the input matrix $X_{n \times m}$ is composed of m pieces of data of dimension n, the data is normalized to the input matrix $X_{n \times m}$, and the covariance matrix is obtained.

$$C_{n \times n} = \frac{1}{m} X_{n \times m} * X_{n \times m}^T \quad (15)$$

Then find the eigenvalues of the covariance matrix and the corresponding eigenvectors:

$$E^T C_{n \times n} E = \Lambda \quad (16)$$

Finally, the eigenvectors are arranged into a matrix from top to bottom according to the size of the corresponding eigenvalues, and the first k rows are taken to form a matrix $W_{k \times n}$, and the data after dimension reduction to k dimension is obtained:

$$Y_{k \times m} = W_{k \times n} * X_{n \times m} \quad (17)$$

In this paper, the wavelet transformed A3, D3, D2, D1 and the original signal S are recombined into a multi-dimensional vector, and then through PCA dimension reduction, the three principal components with the largest contribution rate are retained, and the cumulative contribution rate of the three principal components is 97.77% above, as shown in Fig. 10. It is beneficial to suppress the influence of background noise²², while reducing the input parameters to speed up the calculation.

Dataset construction and algorithm process

Dataset construction

According to the data analysis content of 2.2 in the text, because the line voltage waveform has only a slight fluctuation when the load is working normally, the line voltage waveform when the load is working normally is classified into one category. Since the line voltage waveforms generated by loads with different attributes are different when a series arc fault occurs, the line voltage waveforms when each load fails are marked and distinguished when the samples are constructed. Wavelet decomposition and coefficient reconstruction are performed on the line voltage signal under each type of label, and the reconstructed coefficients A3, D3, D2, D1 and the original signal S are recombined into a multi-dimensional vector, and then the sample dataset is constructed through PCA dimensionality reduction.

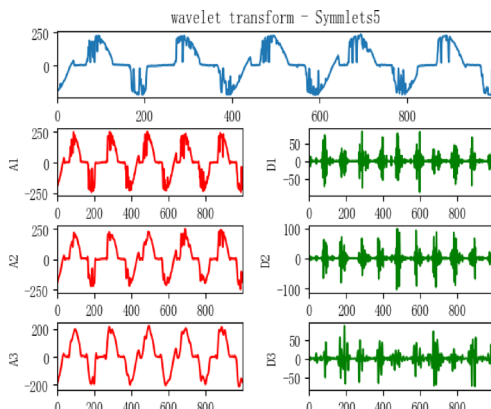


Fig. 9. Wavelet transform.

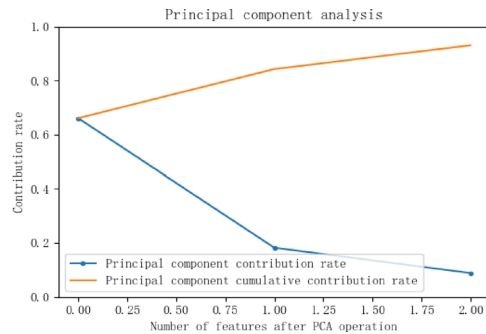


Fig. 10. Principal component contribution rate curve after PCA dimensionality reduction.

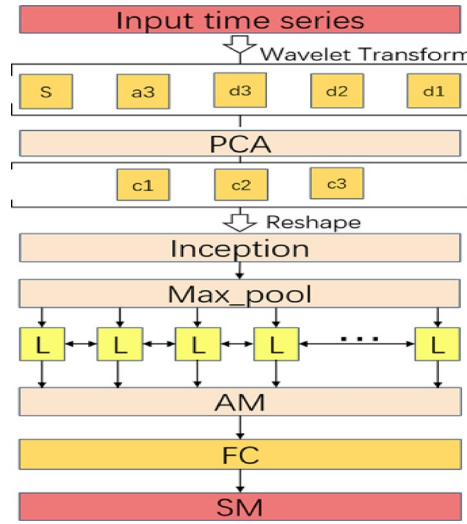


Fig. 11. Flowchart of the algorithm.

Algorithm flowchart

The flow chart of the algorithm proposed in this paper is shown in the Fig. 11 below:

The specific steps can be summarized as:

- Step 1: Build an experimental platform and obtain data, visualize and label the calculated line voltage data, then perform 3-layer wavelet decomposition and single-layer reconstruction, and call PCA dimensionality reduction to construct a sample data set.
- Step 2: The dataset contains a total of 4000 samples. The dataset is randomly scrambled and divided into train set and test set according to the ratio of 7:3.
- Step 3: The samples are imported into the Inception model in batches, and after multi-scale convolution operations, they are used to extract deep-level features under different spatial dimensions.
- Step 4: The two-dimensional vector is adjusted to one-dimensional through the global maximum pooling layer, and imported into the BiLSTM model to extract the feature connections on the previous and previous time steps related to the current moment features.
- Step 5: An improved attention mechanism is introduced into the hidden state vector output to highlight the features that characterize the sample while suppressing the influence of background noise.
- Step 6: The hidden state weighted by the attention weight vector is classified by the fully connected layer and the Softmax layer.

Result analysis

Here, the confusion matrix^{23–25} is used to observe the classification effect of the model after training more intuitively. The vertical axis is the real label, the horizontal axis is the predicted label, and the values on the diagonal represent the probability that the predicted label is the same as the true label, and the remaining values represent the probability that the true label is predicted to be another label.

The Fig. 12 shows the training curve, when the loss value is not higher than 0.15 and the iteration stops when it does not continue to decrease. From the training curve, it can be seen that when the number of iterations is

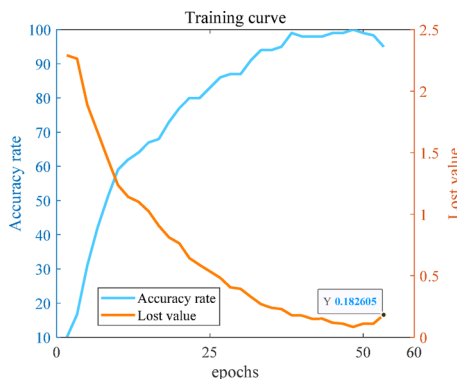


Fig. 12. Training curves.

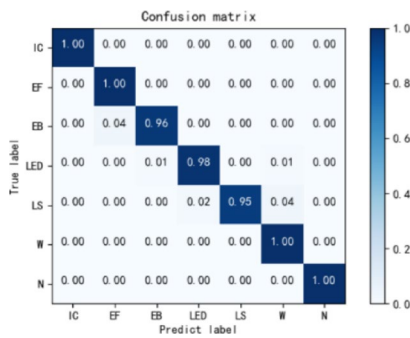


Fig. 13. Confusion matrix of recognition results.

InBiLSTM-A(iba)	Inception-BiLSTM	CNN-LSTM	LSTM
Input (3,1000)	Input (3,1000)	Input (3,1000)	Input (1,1000)
Convolutional layer 1/(1*1) Convolutional layer 2/(1*1)(3*3) Convolutional layer 3/(3*3)(1*1) Convolutional layer 4/(1*1)(3*3)(3*3)	Convolutional layer 1/(1*1) Convolutional layer 2/(1*1)(3*3) Convolutional layer 3/(3*3)(1*1) Convolutional layer 4/(1*1)(3*3)(3*3)	Convolutional layer (3*3)	
Pooling layer(3*3)	Pooling layer (3*3)	pooling layer (3*3)	
BiLSTM layer/8	BiLSTM layer/8	LSTM layer/8	LSTM layer/8
Attention mechanism layer /16			
Fully connected layer /7	Fully connected layer /7	Fully connected layer/7	Fully connected layer /7

Table 2. The structure of each network.

less than 50, the loss value decreases, and when the number of iterations exceeds 50, the loss value increases. Terminate the iteration when the loss value is greater than 0.15.

It can be seen from the Fig. 13 that the algorithm in this paper can effectively identify the arc faults of various loads, and only has a small misjudgment rate for a small number of loads, which shows that the algorithm has excellent performance in the diagnosis of multi-load types of lines.

Comparison of schemes

In order to verify the performance of the model proposed in this paper, it is compared with LSTM, Inception-BiLSTM and CNN-LSTM. The structure of each network is shown in Table 2.

Each network adopts Adam optimization function and cross entropy loss function, the epoch is 50, and the training accuracy curve and AUCROC curves for all models are shown in the Figs. 14 and 15 below.

It can be seen from the AUCROC curve that the AUC value of the model is 0.9823 after the attention mechanism is added, which is 0.162 higher than that without the attention mechanism, and the performance of the model reaches a high level, and the performance of the model is the best among all models.

Compared with the LSTM model, the recognition effect of the network is significantly improved after the convolution module is added, and the recognition accuracy of the deeper and wider convolutional network is better. According to the comparison between the algorithm in this paper and Inception-BiLSTM, it can be

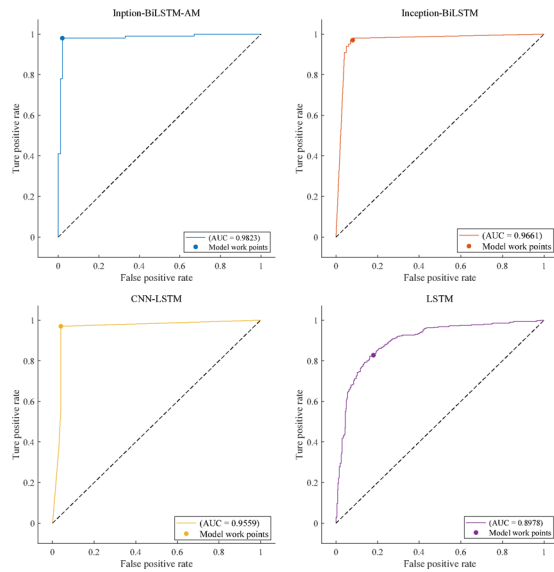


Fig. 14. AUCROC curves for all models.

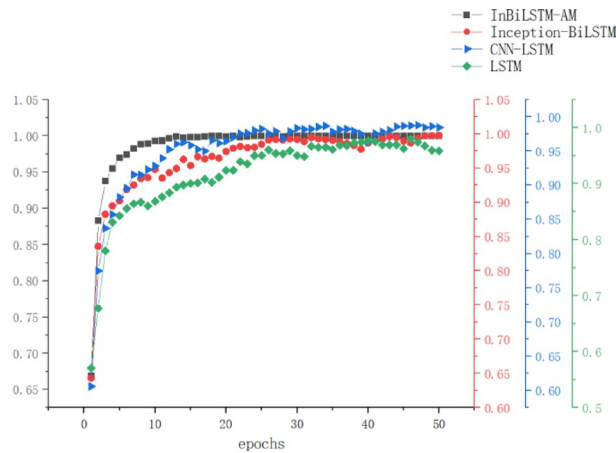


Fig. 15. Comparison of training accuracy curves of each algorithm.

seen that adding the attention mechanism can improve the speed of convergence and the effect of recognition. Therefore, compared with the other three algorithms, this model is more superior in recognition rate and convergence speed, can more quickly and accurately identify the line voltage variation characteristics of household loads, and more effectively detect series arc faults generated in the line.

Different sampling frequency test

In practice, the series arc fault detection device samples the voltage signal through a certain sampling frequency when identifying the arc fault. In order to have a deeper understanding of the impact of the sampling frequency on the accuracy of the series arc fault identification. Through additional experiments, the power supply terminal voltage and load terminal voltage signals at three sampling frequencies of 20 kHz, 5 kHz and 1 kHz were collected, and the dataset was constructed using the same method as above. The series arc fault detection is carried out by the InBiLSTM-AM model. The identification performance under different sampling frequencies is analyzed here using standard error plots for all types of loads. The recognition results are shown in the Fig. 16 below.

Obviously, all four sampling frequencies can produce higher recognition rate, which reflects the good adaptability of the algorithm. At the same time, it can be seen from the comparison that the recognition accuracy is the best when the sampling frequency is 10 kHz, which has certain theoretical guiding significance for the development of the series arc fault detection device.

Engineering RealizatioCNN-LSTM

The development logic of the series arc fault detection device is shown in the Fig. 17 below.

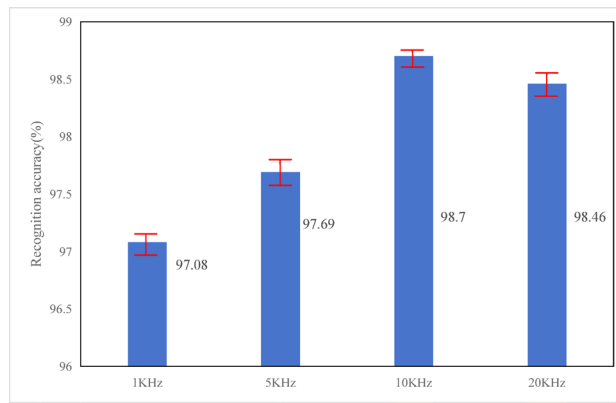


Fig. 16. Comparison of recognition accuracy under different sampling frequencies.

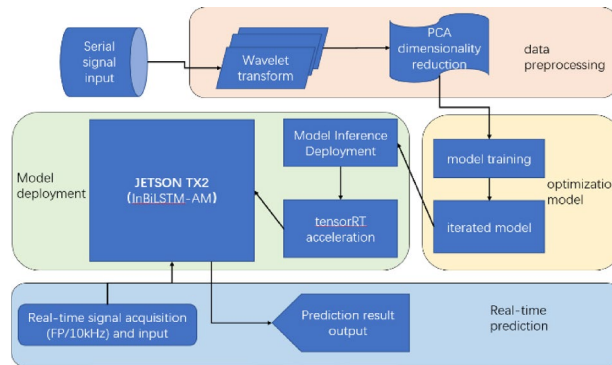


Fig. 17. Logic diagram of detection device.

The first is to import the collected sequence signal after wavelet transform and PCA preprocessing into the model for algorithm training, infer and deploy the trained model to the Jetson TX2 processor. Then use the 10KHZ sampling frequency to collect the real-time voltage signal according to the sensor, and finally import it into the inference model of the processor for prediction and identification. The development and realization of the series arc fault detection device has practical significance and application value for preventing household electrical fires.

Conclusion

Aiming at the difficulty of arc faults detection in series in low-voltage load lines, an experimental platform was built, and the characteristics of relevant voltage data were collected and analyzed. An InBiLSTM-AM model based on wavelet transform and PCA dimensionality reduction is proposed to detect series arc faults, and good identification results are obtained. At the same time, the effectiveness of the algorithm is further demonstrated by horizontal comparison with a variety of algorithms, and the conclusions are as follows.

A series arc fault experiment platform for household loads was built. Through the collected power supply terminal voltage and load side voltage of various load circuits, the line voltage of each load in normal and fault operation was calculated, and preliminarily analyzed the characterizing effect of the line voltage on the arc fault properties of each load.

The voltage of each load line is decomposed and reconstructed by wavelet function, and the characteristics of high frequency and low frequency components of the voltage signal are analyzed from the time-frequency domain. And a preprocessing method is proposed, which is a multi-dimensional matrix composed of the wavelet transformed A3, D3, D2, D1 and the original signal S to form samples through PCA dimensionality reduction.

The InBiLSTM-AM algorithm with attention mechanism is proposed. Compared with the other three algorithms, it is verified that the algorithm has obvious advantages in the recognition rate of low-voltage load arc faults.

Through additional comparison experiments, it is determined that the model detection effect is the best when the sampling frequency is 10 KHZ, which provides a theoretical reference for the development of real-time series arc fault detection devices.

The development logic and engineering realization plan of the series arc fault detection device are preliminarily envisaged, which has practical significance for preventing low-voltage electrical fires.

Data availability

All data generated or analysed during this study are included in this published article and its supplementary information files.

Received: 30 April 2024; Accepted: 18 July 2025

Published online: 27 July 2025

References

- Guo, F. et al. Detection and line selection of series arc fault in multi-load circuit. *IEEE Trans. Plasma Sci.* **47**(11), 5089–5098 (2019).
- Braunovic, M., Konchits, V. V. & Myshkin, N. K. Electrical contact theory. In *Application and Technology* (Machinery Industry Press, Beijing, 2010).
- Vasile, C. & Ioana, C. Arc fault detection and localization by electromagnetic-acoustic remote sensing. In *Proc. RADIO*, 1–2 (Saint-Gilles Les Bains, Reunion Island, 2016).
- Hui, L., Qiongfang, Y., Aihua, D., Qiongfang, Y. & Dezhong, Z. Study on electric arc's on-line detection for low voltage switchbox based on information fusion. In *Proc. ICFN*, V1-204–V1-207 (Sanya, Hainan China, 2010).
- Lezama, J., Schweitzer, P. & Weber, S. Arc fault detection based on temporal analysis. In *Holm* (New Orleans, Louisiana, 2015).
- Momoh, J. A. & Button, R. Design and analysis of aerospace DC arc faults using fast Fourier transformation and artificial neural network. In *PES. GM* 791–792 (Orlando, Florida, 2003).
- Jiang, J. et al. Series arc fault detection based on random forest and deep neural network. *IEEE Sens. J.* **21**(15), 17171–17179 (2021).
- Zhang, S., Qu, N., Zheng, T. & Hu, C. Series arc fault detection based on wavelet compression reconstruction data enhancement and deep residual network. *IEEE Trans. Instrum. Meas.* **71**, 1–9 (2022).
- Long, G., Mu, H., Li, Y., Zhang, D., Ding, N. & Zhang, G. Fault identification technology of series arc based on deep learning algorithm. In *ICHVE*, 1–4 (Beijing, 2020).
- Han, X. et al. Series arc fault detection method based on category recognition and artificial neural network. *Electronics* **9**(9), 1367 (2020).
- Chu, R., Schweitzer, P. & Zhang, R. Series AC arc fault detection method based on high-frequency coupling sensor and convolution neural network. *Sensors* **20**, 4910 (2020).
- Wang, Y. et al. ArcNet Series AC arc fault detection based on raw current and convolutional neural network. *IEEE Trans. Ind. Informat.* **18**(1), 77–86 (2022).
- Yang, K. et al. A novel methodology for series arc fault detection by temporal domain visualization and convolutional neural network. *Sensors* **20**, 162 (2020).
- Li, W., Liu, Y., Li, Y. & Guo, F. Series arc fault diagnosis and line selection method based on recurrent neural network. *IEEE Access* **8**, 177815–177822 (2020).
- Ahmadi, M., Samet, H. & Ghanbari, T. A new method for detecting series arc fault in photovoltaic systems based on the blind-source separation. *IEEE Trans. Industr. Electron.* **67**(6), 5041–5049 (2020).
- Telford, R. D., Galloway, S., Stephen, B. & Elders, I. Diagnosis of series DC arc faults: a machine learning approach. *IEEE Trans. Ind. Informat.* **13**(4), 1598–1609 (2016).
- Momoh, J. A. & Button, R. Design and analysis of aerospace DC arcing faults using fast Fourier transformation and artificial neural network. In *2003 IEEE Power Engine* (IEEE, USA, 2003).
- Graves, A. & Schmidhuber, J. Framewise phoneme classification with bidirectional LSTM and other neural network architectures. In *Elsevier Ltd.GM*, 602–610 (Orlando, Florida, 2005).
- Wadood, A. Intelligent real-time Arabic sign language classification using attention-based inception and BiLSTM. *Comput. Electri. Eng.* **95**, 107395 (2021).
- Zhou, P., Shi, W. & Tian, J. Attention-based bidirectional long short-term memory networks for relation classification. In *Proc at the 54th AMAFCL* (Berlin, 2016).
- Yao, X., Herrera, L., Ji, S., Zou, K. & Wang, J. Characteristic study and time-domain discrete-wavelet-transform based hybrid detection of series DC arc faults. *IEEE Trans. Power Electron.* **29**(6), 3103–3115 (2014).
- Guo, F. et al. Feature extraction method of series arc fault based on ST-SVD-PCA. *J. China Coal Soc* **43**(3), 888–896 (2018).
- Han, C., Wang, Z., Tang, A., Gao, H. & Guo, F. Recognition method of AC series arc fault characteristics under complicated harmonic conditions. *IEEE Trans. Instrum. Meas.* **70**, 1–9 (2021).
- Cheng, C. et al. Enhanced fault diagnosis using broad learning for traction systems in high-speed trains. *IEEE Trans. Power Electron.* **36**(7), 7461–7469 (2021).
- Bao, G., Jiang, R. & Gao, X. Novel series arc fault detector using high-frequency coupling analysis and multi-indicator algorithm. *IEEE Access* **7**, 92161–92170 (2019).

Author contributions

L and S write the manuscript together, and C prepare graphs and tables.

Declarations

Competing interests

The authors declare no competing interests.

Additional information

Supplementary Information The online version contains supplementary material available at <https://doi.org/10.1038/s41598-025-12760-7>.

Correspondence and requests for materials should be addressed to J.S.

Reprints and permissions information is available at www.nature.com/reprints.

Publisher's note Springer Nature remains neutral with regard to jurisdictional claims in published maps and institutional affiliations.

Open Access This article is licensed under a Creative Commons Attribution-NonCommercial-NoDerivatives 4.0 International License, which permits any non-commercial use, sharing, distribution and reproduction in any medium or format, as long as you give appropriate credit to the original author(s) and the source, provide a link to the Creative Commons licence, and indicate if you modified the licensed material. You do not have permission under this licence to share adapted material derived from this article or parts of it. The images or other third party material in this article are included in the article's Creative Commons licence, unless indicated otherwise in a credit line to the material. If material is not included in the article's Creative Commons licence and your intended use is not permitted by statutory regulation or exceeds the permitted use, you will need to obtain permission directly from the copyright holder. To view a copy of this licence, visit <http://creativecommons.org/licenses/by-nc-nd/4.0/>.

© The Author(s) 2025